

Phosphorus–Phosphorus Bond Cleavage in the Cage Molecule P_4S_3 : Synthesis and Crystal Structure of the Trinuclear Platinum Complex $[\{Pt(\mu-P_4S_3)(PPh_3)\}_3]\cdot C_6H_6$ *

Massimo Di Vaira, Maurizio Peruzzini, and Piero Stoppioni

Dipartimento di Chimica, Università, Istituto I.S.S.E.C.C., C.N.R., Via J. Nardi, 39, 50132 Firenze, Italy

The reaction of $[Pt(C_2H_4)(PPh_3)_2]$ with P_4S_3 yielded the trinuclear platinum complex $[\{Pt(\mu-P_4S_3)(PPh_3)\}_3]\cdot C_6H_6$ whose structure has been determined by X-ray diffraction. Crystals are triclinic, space group $P\bar{1}$, with $Z = 2$ in a unit cell of dimensions $a = 21.414(12)$, $b = 15.450(9)$, $c = 15.670(9)$ Å, $\alpha = 121.71(9)$, $\beta = 94.22(8)$, and $\gamma = 107.50(9)^\circ$. The final R factor was 0.069 for 3 990 independent observed reflections. Insertion of a metal–ligand moiety into a P–P bond of the cage molecule occurs and a trinuclear structure is formed by sharing one P atom from such a bond between two Pt atoms. The Pt...Pt separations range from 4.05 to 4.22 Å and the mean P...P distance after cleavage is 3.03(3) Å.

It has been recently found that E_4X_3 ($E = As$ or P , $X = S$ or Se) cage molecules react with appropriate transition metal–ligand moieties to give different products depending on the nature of the metal atom and its oxidation state. In particular, the intact P_4X_3 ($X = S$ or Se) molecules are co-ordinated to the metal through their apical P atom in the d^{10} four-co-ordinate complexes $[M(P_4X_3)(tpea)]$ [$M = Ni$ or Pd , $tpea = tris(2-diphenylphosphinoethyl)amine$].^{1,2} P_4S_3 reacts with $[IrCl(CO)(PPh_3)_2]$ to give the dimeric compound $[\{Ir(\mu-P_4S_3)Cl(CO)(PPh_3)\}_2]$,³ in which cleavage of a P–P bond in the cage molecule has occurred. Reaction of E_4X_3 ($E = As$ or P ; $X = S$ or Se) with rhodium(i) or iridium(i) complexes in the presence of 1,1,1-tris(diphenylphosphinomethyl)ethane (tppme) yields the complexes $[M(E_3X_3)(tppme)]$ ($M = Rh$ or Ir ; $E = P$, $X = S$ or Se ; $E = As$, $X = S$) in which an atom in the base of the cage has been replaced by the $M(tppme)$ moiety.⁴ More substantial cleavage of the cage molecules occurs in reactions with cobalt(ii) and nickel(ii) tetrafluoroborate in the presence of tppme which afford complexes containing heterocyclic E_2X ($E = P$ or As , $X = S$ or Se)^{5,6} or homocyclic E_3 ($E = P$ or As)^{7,8} units η^3 -bonded to the metal atom.

The above results suggest that metal-assisted cleavage of bonds in the cage molecule is related both to the initial electron count on the metal atom and to the geometry-determined bonding mode of the specific metal–ligand system provided by the reactant. Since interaction with the d^{10} $M(tpea)$ metal moiety in the C_{3v} symmetry imposed by the tripod-like tpea ligand had been found to preserve the cage molecule,^{1,2} we have investigated the reaction of P_4S_3 with a d^{10} metal complex containing unidentate phosphines and thus providing a different environment from that of tpea. The reaction of P_4S_3 with $[Pt(C_2H_4)(PPh_3)_2]$ yielded the trinuclear complex $[\{Pt(\mu-P_4S_3)(PPh_3)\}_3]\cdot C_6H_6$ whose structure has been established by a single-crystal X-ray diffraction study.

Experimental

All solvents were reagent grade and were dried by distillation from suitable agents.⁹ All reactions and manipulations were

carried out under dry nitrogen. The P_4S_3 was purchased from Fluka (AG) and used after recrystallization from benzene; $[Pt(C_2H_4)(PPh_3)_2]$ was prepared by the published procedure.¹⁰ Mass spectra were recorded on a Kratos MS 80 mass spectrometer with an ionizing voltage of 70 eV ($\approx 1.1 \times 10^{-17}$ J). A direct insertion probe was employed with the source temperature ranging from 100 to 280 °C.

Preparation of $[\{Pt(\mu-P_4S_3)(PPh_3)\}_3]\cdot C_6H_6$.— P_4S_3 (0.5 mmol) dissolved in benzene (30 cm³) was slowly added to a solution of $[Pt(C_2H_4)(PPh_3)_2]$ (0.5 mmol) in acetone (70 cm³) at 0 °C; during the addition the solution turned red initially and then a finely powdered precipitate separated out. As soon as the addition of P_4S_3 was complete the reaction flask was closed and the resulting suspension left overnight at room temperature to give red crystals of the compound. The crystals were separated from the powdered precipitate by decantation with benzene and light petroleum (40–70 °C), then filtered on a sintered glass frit, and dried in a stream of inert gas (yield ca. 25–30%) (Found: C, 34.05; H, 2.30; P, 21.75; S, 13.20. $C_{54}H_{45}P_{15}Pt_3S_9\cdot C_6H_6$ requires C, 34.15; H, 2.45; P, 22.00; S, 13.65%).

Collection and Reduction of X-Ray Data.—Crystals of $[\{Pt(\mu-P_4S_3)(PPh_3)\}_3]\cdot C_6H_6$ did not provide good material for X-ray diffraction due to their small size and to disorder, whose amount varied from sample to sample. Practically no intensities could be recorded at $2\theta > 40^\circ$ using Mo- K_α radiation. The crystal used for the final data collection had dimensions ca. 0.10 × 0.05 × 0.05 mm. A Philips PW 1100 automated diffractometer and graphite-monochromated Mo- K_α radiation were used throughout. Unit-cell dimensions were determined by least-squares refinement of the angular settings of 24 reflections with $20 < 2\theta < 30^\circ$. Intensity data were collected at room temperature in the range $5 < 2\theta < 40^\circ$ by the θ – 2θ scan technique, with a symmetric scan range of $(1.10 + 0.30 \tan\theta)^\circ$ and a scan speed of 5.0° min⁻¹ in 2θ . Stationary background counts were taken at each end of the scan for fixed 3-s intervals. The intensities of three standard reflections, well separated in reciprocal space, were monitored periodically throughout the data collection and showed only random variations ($< \pm 1.5\%$) in the mean values. Corrections for Lorentz, polarization, and X-ray absorption effects were applied. 3 990 Unique reflections having $I > 3\sigma(I)$ were used in the solution and refinement of the structure.

Crystal Data. $C_{60}H_{51}P_{15}Pt_3S_9$, $M = 2\ 110.53$, triclinic, space group $P\bar{1}$, $a = 21.414(12)$, $b = 15.450(9)$, $c = 15.670(9)$ Å, $\alpha = 121.71(9)$, $\beta = 94.22(8)$, $\gamma = 107.50(9)^\circ$, $U = 4\ 031.2$ Å³,

* Tris(2,6,7-trithia-1,3,4,5-tetraphosphabicyclo[2.2.1]heptane-3,5-diyl- $P^2, \mu-P^3$)tris(triphenylphosphineplatinum)–benzene (1/1).

Supplementary data available (No. SUP 56083, 5 pp.); thermal parameters, H-atom co-ordinates. See Instructions for Authors, *J. Chem. Soc., Dalton Trans.*, 1985, Issue 1, pp. xvii–xix. Structure factors are available from the editorial office.

Table 1. Atomic co-ordinates^{a,b} ($\times 10^4$) for $[\{\text{Pt}(\mu\text{-P}_4\text{S}_3)(\text{PPh}_3)_2\}_3]\cdot\text{C}_6\text{H}_6$

Atom	x	y	z	Atom	x	y	z
Pt(1)	7 830(1)	1 423(1)	6 199(1)	C(36)	10 269(9)	2 527(20)	7 368(16)
Pt(2)	7 161(1)	3 326(1)	5 652(1)	C(41)	7 851(12)	5 201(22)	8 324(21)
Pt(3)	7 090(1)	428(1)	3 115(1)	C(42)	7 976(12)	6 093(22)	9 352(21)
P(1)	8 839(5)	1 424(8)	6 887(7)	C(43)	8 588(12)	6 535(22)	10 098(21)
P(2)	7 088(6)	4 656(9)	7 271(8)	C(44)	9 074(12)	6 084(22)	9 816(21)
P(3)	6 403(5)	121(8)	1 686(7)	C(45)	8 949(12)	5 192(22)	8 788(21)
P(11)	5 732(6)	-175(9)	5 731(8)	C(46)	8 337(12)	4 750(22)	8 043(21)
P(12)	7 340(5)	1 357(9)	7 470(7)	C(51)	7 159(13)	5 959(22)	7 433(20)
P(13)	6 755(6)	2 335(9)	7 496(7)	C(52)	6 565(13)	6 019(22)	7 083(20)
P(14)	6 948(5)	1 930(7)	5 980(7)	C(53)	6 595(13)	6 993(22)	7 202(20)
P(21)	8 875(7)	4 505(10)	4 774(10)	C(54)	7 219(13)	7 906(22)	7 671(20)
P(22)	7 364(7)	4 577(9)	5 172(8)	C(55)	7 812(13)	7 846(22)	8 021(20)
P(23)	7 298(7)	3 301(9)	3 531(8)	C(56)	7 782(13)	7 782(22)	7 902(20)
P(24)	7 434(5)	2 351(7)	4 136(7)	C(61)	6 321(12)	4 247(20)	7 596(18)
P(31)	8 436(6)	-1 204(9)	2 811(8)	C(62)	6 273(12)	4 665(20)	8 612(18)
P(32)	6 805(6)	-1 475(9)	2 293(8)	C(63)	5 641(12)	4 320(20)	8 778(18)
P(33)	7 173(6)	-1 235(8)	3 795(7)	C(64)	5 057(12)	3 727(20)	7 927(18)
P(34)	7 788(5)	540(7)	4 415(7)	C(65)	5 105(12)	3 139(20)	6 911(18)
S(11)	6 565(5)	-293(9)	6 358(8)	C(66)	5 737(12)	3 484(20)	6 745(18)
S(12)	5 754(5)	1 292(10)	7 094(8)	C(71)	5 863(12)	913(19)	2 083(17)
S(13)	6 071(5)	475(8)	4 862(7)	C(72)	5 647(12)	1 124(19)	2 966(17)
S(21)	8 429(7)	5 503(9)	5 801(9)	C(73)	5 226(12)	1 705(19)	3 278(17)
S(22)	8 229(7)	3 932(10)	3 346(9)	C(74)	5 022(12)	2 075(19)	2 708(17)
S(23)	8 540(6)	3 030(9)	4 681(8)	C(75)	5 239(12)	1 864(19)	1 826(17)
S(31)	7 618(6)	-1 717(9)	1 597(7)	C(76)	5 659(12)	1 283(19)	1 513(17)
S(32)	7 902(6)	-1 914(9)	3 539(8)	C(81)	5 785(9)	-1 314(20)	726(18)
S(33)	8 698(5)	484(8)	3 970(7)	C(82)	6 000(9)	-2 075(20)	-34(18)
C(11)	8 882(11)	52(17)	6 265(17)	C(83)	5 555(9)	-3 191(20)	-712(18)
C(12)	9 408(11)	-177(17)	5 835(17)	C(84)	4 896(9)	-3 545(20)	-630(18)
C(13)	9 422(11)	-1 222(17)	5 401(17)	C(85)	4 681(9)	-2 784(20)	130(18)
C(14)	8 910(11)	-2 037(17)	5 397(17)	C(86)	5 126(9)	-1 668(20)	808(18)
C(15)	8 385(11)	-1 807(17)	5 827(17)	C(91)	6 867(11)	472(19)	911(13)
C(16)	8 371(11)	-763(17)	6 261(17)	C(92)	7 578(11)	1 000(19)	1 272(13)
C(21)	9 006(12)	1 956(20)	8 274(19)	C(93)	7 947(11)	1 216(19)	659(13)
C(22)	8 944(12)	2 958(20)	8 934(19)	C(94)	7 604(11)	905(19)	-314(13)
C(23)	9 120(12)	3 476(20)	10 014(19)	C(95)	6 893(11)	376(19)	-674(13)
C(24)	9 357(12)	2 993(20)	10 433(19)	C(96)	6 524(11)	160(19)	-62(13)
C(25)	9 419(12)	1 990(20)	9 774(19)	C(101)	7 375(13)	3 455(21)	388(19)
C(26)	9 244(12)	1 471(20)	8 694(19)	C(102)	7 107(13)	3 363(21)	1 135(19)
C(31)	9 615(9)	2 365(20)	6 938(16)	C(103)	6 906(13)	4 180(21)	1 851(19)
C(32)	9 535(9)	2 991(20)	6 578(16)	C(104)	6 973(13)	5 088(21)	1 820(19)
C(33)	10 108(9)	3 781(20)	6 648(16)	C(105)	7 240(13)	5 180(21)	1 072(19)
C(34)	10 762(9)	3 944(20)	7 078(16)	C(106)	7 441(13)	4 363(21)	356(19)
C(35)	10 842(9)	3 317(20)	7 438(16)				

^a Estimated standard deviations in this and other Tables are given in parentheses. ^b Atoms C(101)—C(106) belong to the benzene solvate molecule.

$F(000) = 2\,028$, $D_c = 1.738\text{ g cm}^{-3}$, $Z = 2$, Mo-K_α radiation, $\lambda = 0.710\,69\text{ \AA}$, $\mu(\text{Mo-K}_\alpha) = 57.98\text{ cm}^{-1}$.

Structure solution and refinement. The structure was solved by a combination of heavy-atom and direct methods which provided the positions of the metal atoms. The other non-hydrogen atoms were located from subsequent Fourier maps. In the full-matrix least-squares refinement [314 parameters; function $\sum w(|F_o| - |F_c|)^2$ minimized, with weights $w = 1/\sigma^2(F_o)$] the Pt, P, and S atoms were assigned anisotropic thermal parameters. The phenyl groups and the solvate benzene molecule were refined as rigid groups with idealized geometry, each being assigned an overall thermal parameter. Hydrogen atoms were introduced in calculated positions ($\text{C-H} = 1.00\text{ \AA}$) with thermal parameters 20% larger than those of the respective carbon atoms. Scattering factors for the neutral atoms were taken from ref. 11 and the anomalous dispersion correction for Pt from ref. 12. The final values of the discrepancy indices were $R = \Sigma(|F_o| - |F_c|)/\Sigma|F_o| = 0.069$ and $R' = [\Sigma w(|F_o| - |F_c|)^2/\Sigma w(F_o^2)]^{1/2} = 0.068$. No shift-to-error ratio in the final cycle was larger than 0.01. The highest peaks in the final difference-Fourier map, with heights $< 1.7\text{ e \AA}^{-3}$, were close to

the positions of the Pt atoms. Computations used the SHELX system¹³ and the Figures were constructed using ORTEP-II,¹⁴ both implemented on a SEL 32/70 computer by Dr. C. Mealli. The final positional parameters for the non-hydrogen atoms are listed in Table 1.

Results and Discussion

The reaction of $[\text{Pt}(\text{C}_2\text{H}_4)(\text{PPh}_3)_2]$ with tetraphosphorus trisulphide, P_4S_3 , affords a compound of formula $[\{\text{Pt}(\mu\text{-P}_4\text{S}_3)(\text{PPh}_3)_2\}_3]$. Analytical data for the complex, which crystallizes with one molecule of benzene, are in good agreement with this formula. The compound, which is air stable in the solid state for several days, is insoluble in all organic solvents with the exception of carbon disulphide in which it undergoes decomposition even under nitrogen. The mass spectrum shows, up to ca. 280°C , only the peaks of the triphenylphosphine ligand, in addition to those of the benzene solvate molecule.

The structure of the compound consists of trinuclear $[\{\text{Pt}(\mu\text{-P}_4\text{S}_3)(\text{PPh}_3)_2\}_3]$ molecules, which possess no symmetry element, and benzene solvate molecules. A schematic repre-

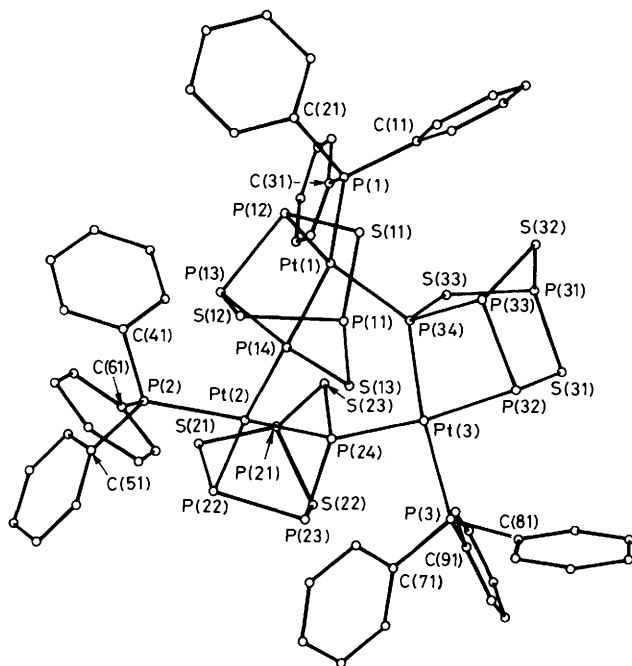


Figure 1. A view of the $[\{\text{Pt}(\mu\text{-P}_4\text{S}_3)(\text{PPh}_3)_3\}_3]$ molecule. Only the first carbon atom of each phenyl group is labelled

sensation of the trinuclear molecule is shown in Figure 1 and a view of its inner skeleton is shown in Figure 2. Values of bond distances and angles are given in Table 2.

In each of the chemically identical $\text{Pt}(\mu\text{-P}_4\text{S}_3)(\text{PPh}_3)_3$ units the metal atom is linked to two 'basal' phosphorus atoms of the P_4S_3 cage which lie much farther apart than in free P_4S_3 [$3.03(3) \text{ \AA}$ vs. $2.235(11) \text{ \AA}$ ¹⁵ (mean values)]. One of these P atoms is also bonded to a Pt atom of another $\text{Pt}(\mu\text{-P}_4\text{S}_3)(\text{PPh}_3)_3$ unit so that each of the metal atoms, which are four-coordinate, is bound to three P_4S_3 phosphorus atoms, belonging to two different cages, and to one phosphine P atom. The formation of the trinuclear compound therefore involves loss of C_2H_4 and one PPh_3 ligand from each molecule of the reactant, $[\text{Pt}(\text{C}_2\text{H}_4)(\text{PPh}_3)_2]_2$, as well as insertion of a $\text{LL}'\text{Pt}$ moiety into a P–P bond of the P_4S_3 molecule. Such a process is analogous to that³ which leads to the formation of the dinuclear complex $[\{\text{Ir}(\mu\text{-P}_4\text{S}_3)\text{Cl}(\text{CO})(\text{PPh}_3)_2\}_2]$, where a metal moiety with different geometry and *d*-electron count than the present $\text{LL}'\text{Pt}$ one, but isolobal with it,¹⁶ inserts into a P–P bond of the P_4S_3 cage. Such a bond lengthens to $3.055(5) \text{ \AA}$, a distance comparable to that found in the present Pt derivative. The long Pt...Pt distances ($4.05\text{--}4.22 \text{ \AA}$) exclude the existence of any direct metal–metal interaction.

The co-ordination geometry of two of the Pt atoms is nearly planar but that of the third Pt atom is rather distorted from planarity, as indicated by the values of the dihedral angles between the four planes defined by pairs of *cis*-Pt–P bonds about each metal centre. Such angles are large about Pt(2) and Pt(3), 176.6 and 171.3° respectively, but are as small as 146.5° about Pt(1). The six-membered ring formed by the three Pt and three bridging P atoms in the core of the molecule is not planar. Moreover, it is rather asymmetrical as (a) one P atom lies on the opposite side to the others with respect to the plane passing through the Pt atoms (Figure 2), and (b) the angles between the latter plane and the planes through the Pt–P–Pt fragments in the ring span a wide range, being 94.7 , 123.6 , and 148.1° for the fragments containing P(14), P(24), and P(34), respectively. Consequently, the arrangement of the P_4S_3 moieties is not

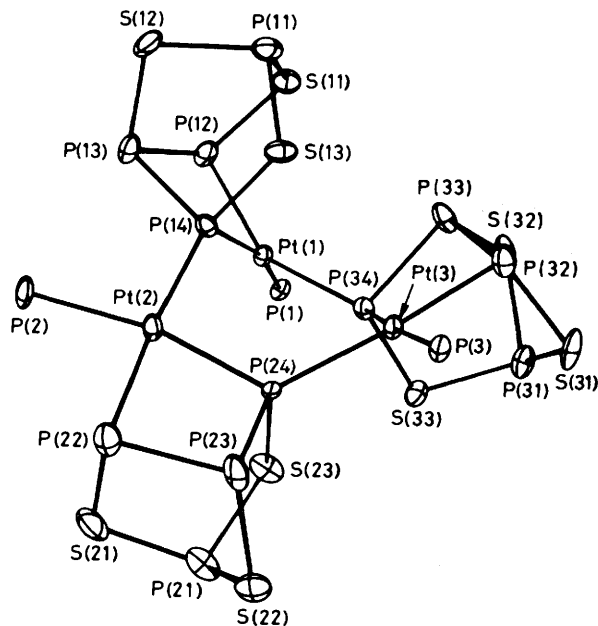
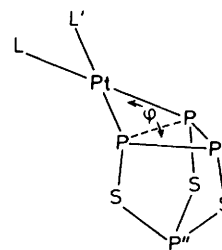


Figure 2. Inner skeleton of the $[\{\text{Pt}(\mu\text{-P}_4\text{S}_3)(\text{PPh}_3)_3\}_3]$ molecule



Scheme.

regular, two of the cages pointing in opposite directions, away from the plane through the metal atoms, whereas the third lies essentially in that plane (Figure 2).

In spite of such differences in arrangement, the three cages have essentially similar dimensions, the largest differences between their corresponding bond lengths and angles (*ca.* 0.05 \AA and 3° , respectively) being less than five times the standard deviation on individual values. Insertion of the metal–ligand moiety into the P–P bond induces minor variations in bond distances within the P_4S_3 cluster: the largest changes from the free P_4S_3 molecule involve the P–S bonds formed by the P atoms bound to Pt, with an increase in the mean from $2.093(3) \text{ \AA}$ ¹⁵ to $2.14(2) \text{ \AA}$. Changes in bond angles upon insertion are obviously more substantial, the largest affecting the P–P'–P angle in the base of the cage (Scheme), which opens from a mean value of 60 to $86.0(6)^\circ$ [*cf.* $84.8(2)^\circ$ in the dimeric Ir derivative³]. The 'hinge' dihedral angle, ϕ , between the above three-phosphorus plane and the plane defined by Pt and two P atoms as shown in the Scheme spans the range $152.2\text{--}157.7^\circ$, which is rather narrow considering the different orientations of the cages in the trinuclear molecule.

In an attempt to rationalize geometrical features such as that mentioned above and to understand the nature of factors controlling the insertion of the metal moiety into the cage, extended Hückel calculations¹⁷ with parameters and procedures specified in the literature¹⁶ were undertaken on an idealized $\text{Pt}(\text{P}_4\text{S}_3)(\text{PH}_3)_2$ model of the monomeric unit ($\text{L} = \text{L}'$ in the Scheme), whose geometry at various stages of the insertion process was

Table 2. Bond lengths (Å) and angles (°) for $[\{\text{Pt}(\mu\text{-P}_4\text{S}_3)(\text{PPh}_3)\}_3]\text{-C}_6\text{H}_6$ *

Pt(1)-P(1)	2.34(1)	Pt(2)-P(2)	2.34(1)	Pt(3)-P(3)	2.32(1)
Pt(1)-P(12)	2.35(1)	Pt(2)-P(22)	2.36(1)	Pt(3)-P(32)	2.35(1)
Pt(1)-P(14)	2.32(1)	Pt(2)-P(24)	2.29(1)	Pt(3)-P(34)	2.33(1)
Pt(1)-P(34)	2.36(1)	Pt(2)-P(14)	2.39(1)	Pt(3)-P(24)	2.33(1)
P(12)-P(13)	2.22(1)	P(22)-P(23)	2.23(1)	P(32)-P(33)	2.22(1)
P(13)-P(14)	2.22(1)	P(23)-P(24)	2.20(1)	P(33)-P(34)	2.24(1)
P(12)-S(11)	2.16(2)	P(22)-S(21)	2.11(2)	P(32)-S(31)	2.15(2)
P(13)-S(12)	2.06(2)	P(23)-S(22)	2.06(2)	P(33)-S(32)	2.08(2)
P(14)-S(13)	2.12(1)	P(24)-S(23)	2.17(1)	P(34)-S(33)	2.13(1)
P(11)-S(11)	2.08(2)	P(21)-S(21)	2.09(2)	P(31)-S(31)	2.10(2)
P(11)-S(12)	2.13(2)	P(21)-S(22)	2.10(2)	P(31)-S(32)	2.14(2)
P(11)-S(13)	2.13(1)	P(21)-S(23)	2.09(2)	P(31)-S(33)	2.10(1)
P(1)-C(11)	1.85(3)	P(2)-C(41)	1.85(3)	P(3)-C(71)	1.84(2)
P(1)-C(21)	1.83(2)	P(2)-C(51)	1.85(3)	P(3)-C(81)	1.83(2)
P(1)-C(31)	1.81(2)	P(2)-C(61)	1.79(3)	P(3)-C(91)	1.82(2)
P(12)···P(14)	3.04(1)	P(22)···P(24)	3.00(1)	P(32)···P(34)	3.05(1)
Pt(1)···Pt(2)	4.05(1)	Pt(2)···Pt(3)	4.08(1)	Pt(3)···Pt(1)	4.22(1)
P(1)-Pt(1)-P(12)	92.4(3)	P(2)-Pt(2)-P(22)	90.4(4)	P(3)-Pt(3)-P(32)	92.5(3)
P(1)-Pt(1)-P(14)	163.1(3)	P(2)-Pt(2)-P(24)	167.3(4)	P(3)-Pt(3)-P(34)	173.4(3)
P(1)-Pt(1)-P(34)	101.4(3)	P(2)-Pt(2)-P(14)	94.7(3)	P(3)-Pt(3)-P(24)	94.9(3)
P(12)-Pt(1)-P(14)	81.3(3)	P(22)-Pt(2)-P(24)	80.3(3)	P(32)-Pt(3)-P(34)	81.5(3)
P(12)-Pt(1)-P(34)	147.7(4)	P(22)-Pt(2)-P(14)	174.8(3)	P(32)-Pt(3)-P(24)	172.4(3)
P(14)-Pt(1)-P(34)	91.9(3)	P(24)-Pt(2)-P(14)	94.8(3)	P(34)-Pt(3)-P(24)	91.2(3)
Pt(1)-P(12)-P(13)	93.2(4)	Pt(2)-P(22)-P(23)	93.3(5)	Pt(3)-P(32)-P(33)	92.6(4)
Pt(1)-P(12)-S(11)	94.0(4)	Pt(2)-P(22)-S(21)	103.4(6)	Pt(3)-P(32)-S(31)	102.5(5)
P(13)-P(12)-S(11)	99.3(6)	P(23)-P(22)-S(21)	100.6(7)	P(33)-P(32)-S(31)	102.1(6)
P(12)-P(13)-P(14)	86.5(5)	P(22)-P(23)-P(24)	85.2(5)	P(32)-P(33)-P(34)	86.3(5)
P(12)-P(13)-S(12)	103.6(6)	P(22)-P(23)-S(22)	104.6(7)	P(32)-P(33)-S(32)	103.8(6)
P(14)-P(13)-S(12)	104.7(6)	P(24)-P(23)-S(22)	105.0(7)	P(34)-P(33)-S(32)	102.9(6)
Pt(1)-P(14)-P(13)	94.0(4)	Pt(2)-P(24)-P(23)	96.3(4)	Pt(3)-P(34)-P(33)	92.3(4)
Pt(1)-P(14)-Pt(2)	118.6(4)	Pt(2)-P(24)-Pt(3)	124.2(4)	Pt(3)-P(34)-Pt(1)	128.3(4)
Pt(1)-P(14)-S(13)	108.7(5)	Pt(2)-P(24)-S(23)	101.9(5)	Pt(3)-P(34)-S(33)	105.8(4)
P(13)-P(14)-Pt(1)	118.0(5)	P(23)-P(24)-Pt(3)	124.4(5)	P(33)-P(34)-Pt(1)	100.4(4)
P(13)-P(14)-S(13)	103.0(5)	P(23)-P(24)-S(23)	100.5(6)	P(33)-P(34)-S(33)	102.8(5)
Pt(2)-P(14)-S(13)	112.2(5)	Pt(3)-P(24)-S(23)	105.4(5)	Pt(1)-P(34)-S(33)	119.4(5)
P(11)-S(11)-P(12)	108.6(6)	P(21)-S(21)-P(22)	106.4(7)	P(31)-S(31)-P(32)	105.3(6)
P(11)-S(12)-P(13)	99.4(5)	P(21)-S(22)-P(23)	99.7(6)	P(31)-S(32)-P(33)	99.1(6)
P(11)-S(13)-P(14)	102.2(5)	P(21)-S(23)-P(24)	105.2(6)	P(31)-S(33)-P(34)	104.4(6)
S(11)-P(11)-S(12)	99.0(6)	S(21)-P(21)-S(22)	99.1(8)	S(31)-P(31)-S(32)	100.0(7)
S(11)-P(11)-S(13)	106.4(6)	S(21)-P(21)-S(23)	106.8(7)	S(31)-P(31)-S(33)	107.4(6)
S(12)-P(11)-S(13)	99.2(6)	S(22)-P(21)-S(23)	98.9(7)	S(32)-P(31)-S(33)	99.7(6)
Pt(1)-P(1)-C(11)	115.6(8)	Pt(2)-P(2)-C(41)	110.3(8)	Pt(3)-P(3)-C(71)	111.7(7)
Pt(1)-P(1)-C(21)	114.0(8)	Pt(2)-P(2)-C(51)	114.2(9)	Pt(3)-P(3)-C(81)	115.5(8)
Pt(1)-P(1)-C(31)	114.6(8)	Pt(2)-P(2)-C(61)	116.2(9)	Pt(3)-P(3)-C(91)	114.5(8)
C(11)-P(1)-C(21)	103(1)	C(41)-P(2)-C(51)	100(1)	C(71)-P(3)-C(81)	103(1)
C(11)-P(1)-C(31)	108(1)	C(41)-P(2)-C(61)	111(1)	C(71)-P(3)-C(91)	107(1)
C(21)-P(1)-C(31)	100(1)	C(51)-P(2)-C(61)	104(1)	C(81)-P(3)-C(91)	104(1)

* Idealized D_{6h} geometry imposed on phenyl groups and benzene molecule with C-C = 1.395 Å.

based on the present structural data and those for the free cage molecule.¹⁵ The Pt-P distances were not changed during P-P bond cleaving and ϕ (Scheme) was fixed at 155.7°, C_s symmetry being assumed throughout. The insertion was found to be controlled by the interaction between the well known b_2 highest occupied molecular orbital of the PtL_2 fragment¹⁸ and the lowest unoccupied molecular orbital of the P_4S_3 fragment (on top of destabilizing interactions with filled cage orbitals), which is considerably stabilized in the course of the deformation and rehybridizes properly for interaction. Such a mechanism is similar to that already discussed for bond cleaving in substituted cyclopropenium ions.¹⁹ Both the overlap between the above fragment orbitals and the Pt-P overlap population maximize in close proximity of the experimental geometry. At that geometry the overlap population of the P-P bond (Scheme) practically vanishes. The computed value for the hinge angle (from calculations in which only ϕ was varied with P···P fixed at 3.03 Å), corresponding to the minimum in a rather flat total-

energy surface as well as to the maximum of a smoothly varying Pt-P overlap population function, falls in the range 151–156°, close to that of the experimental values. The geometry of the monomer seems therefore to be determined by requirements of largest overlaps and least strains within the monomer itself. On the other hand, the best direction for addition of a planar PtL_3 moiety to one of the P atoms in the Scheme (model for a further step in the formation of the polynuclear compound) is calculated by the above energy and overlap population criteria to occur at a Pt-P-Pt angle *ca.* 20° smaller than the experimental 123.7° (mean over the six-membered ring). The computed value is however close to the 100.8(1)° found for the dinuclear Ir derivative.³ It would therefore appear that formation of the six-membered ring in the present compound involves larger strains, probably released in part by puckering, than the formation of the four-membered ring in the dimeric compound. Nevertheless, the fact that according to the mass spectral data (see above) the core of the trinuclear compound

does not undergo fragmentation up to *ca.* 280 °C is indicative of considerable stability. It should be noted in contrast that the σ -bonded cage molecule is released above 150 °C by the $[M(P_4X_3)(tppea)]$ ($M = Ni, X = S$ or $Se; M = Pd, X = S$) complexes¹ and fragmentation of the free P_4X_3 molecules takes place at even lower temperatures.²⁰

Finally, experimental evidence for oxidation of the metal on adduct formation has been reported in the case of the iridium compound.³ The same point of view should hold in the present case, even in absence of direct experimental evidence, to the extent that empty orbitals of the cage molecule are populated in the course of P-P bond cleavage and oxidation of the metal may be assumed to occur.

Acknowledgements

Thanks are expressed to Professor L. Sacconi for his interest in this work.

References

- 1 M. Di Vaira, M. Peruzzini, and P. Stoppioni, *Inorg. Chem.*, 1983, **22**, 2196.
- 2 M. Di Vaira, M. Peruzzini, and P. Stoppioni, *J. Organomet. Chem.*, 1983, **258**, 373.
- 3 C. A. Chilardi, S. Midollini, and A. Orlandini, *Angew. Chem., Int. Ed. Engl.*, 1983, **22**, 790.
- 4 M. Di Vaira, M. Peruzzini, and P. Stoppioni, *J. Chem. Soc., Chem. Commun.*, 1983, 903.
- 5 M. Di Vaira, M. Peruzzini, and P. Stoppioni, *J. Chem. Soc., Chem. Commun.*, 1982, 894; *J. Chem. Soc., Dalton Trans.*, 1984, 359.
- 6 M. Di Vaira, P. Innocenti, S. Moneti, M. Peruzzini, and P. Stoppioni, *Inorg. Chim. Acta*, 1984, **83**, 161.
- 7 M. Di Vaira, L. Sacconi, and P. Stoppioni, *J. Organomet. Chem.*, 1983, **250**, 183.
- 8 P. Stoppioni and M. Peruzzini, *J. Organomet. Chem.*, 1984, **262**, C5.
- 9 O. O. Perrin, W. L. F. Armarego, and D. R. Perrin, 'Purification of Laboratory Chemicals,' Pergamon Press, Oxford, 1966.
- 10 U. Nagel, *Chem. Ber.*, 1982, **115**, 1998.
- 11 'International Tables for X-Ray Crystallography,' Kynoch Press, Birmingham, 1974, vol. 4.
- 12 Ref. 11, p. 148 *et seq.*
- 13 G. M. Sheldrick, SHELX 76, University Chemical Laboratory, Cambridge, 1976.
- 14 C. K. Johnson, ORTEP-II, Report ORNL-5138, Oak Ridge National Laboratory, Tennessee, 1976.
- 15 Y. C. Leung, J. Waser, S. Van Houten, A. Vos, G. A. Weigers, and E. H. Wiebenga, *Acta Crystallogr.*, 1957, **10**, 574.
- 16 R. Hoffmann, *Angew. Chem., Int. Ed. Engl.*, 1982, **21**, 711 and refs. therein.
- 17 R. Hoffmann, *J. Chem. Phys.*, 1963, **39**, 1397.
- 18 T. A. Albright, R. Hoffmann, J. C. Thibeault, and D. L. Thorn, *J. Am. Chem. Soc.*, 1979, **101**, 3801.
- 19 E. D. Jemmis and R. Hoffmann, *J. Am. Chem. Soc.*, 1980, **102**, 2570.
- 20 G. J. Penney and G. M. Sheldrick, *J. Chem. Soc. A*, 1971, 243.

Received 1st June 1984; Paper 4/902